

Marta Ferraroni,<sup>a\*</sup> Andrea Scozzafava,<sup>a</sup> Sana Ullah,<sup>b</sup> Thierry Tron,<sup>b</sup> Alessandra Piscitelli<sup>c</sup> and Giovanni Sannia<sup>c</sup>

<sup>a</sup>Dipartimento di Chimica 'Ugo Schiff', Università di Firenze, Via della Lastruccia 3, 50019 Sesto Fiorentino (FI), Italy, <sup>b</sup>Laboratoire Biosciences, Institut des Sciences Moléculaires de Marseille, Université Aix-Marseille, ISM2 CNRS UMR 6263, Marseille CEDEX 20, France, and <sup>c</sup>Dipartimento di Scienze Chimiche, Università di Napoli 'Federico II', Via Cintia 4, 80126 Naples, Italy

Correspondence e-mail: marta.ferraroni@unifi.it

Received 2 October 2013

Accepted 3 December 2013

## Crystallization and preliminary X-ray crystallographic analysis of the small subunit of the heterodimeric laccase POXA3b from *Pleurotus ostreatus*

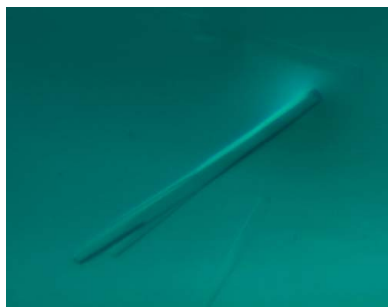
Laccases are multicopper oxidases of great biotechnological potential. While laccases are generally monomeric glycoproteins, the white-rot fungus *Pleurotus ostreatus* produces two closely related heterodimeric isoenzymes composed of a large subunit, homologous to the other fungal laccases, and a small subunit. The sequence of the small subunit does not show significant homology to any other protein or domain of known function and consequently its function is unknown. The highest similarity to proteins of known structure is to a putative enoyl-CoA hydratase/isomerase from *Acinetobacter baumannii*, which shows an identity of 27.8%. Diffraction-quality crystals of the small subunit of the heterodimeric laccase POXA3b (sPOXA3b) from *P. ostreatus* were obtained using the sitting-drop vapour-diffusion method at 294 K from a solution consisting of 1.8 M sodium formate, 0.1 M Tris-HCl pH 8.5. The crystals belonged to the tetragonal space group  $P4_12_12$  or  $P4_32_12$ , with unit-cell parameters  $a = 126.6$ ,  $c = 53.9$  Å. The asymmetric unit contains two molecules related by a noncrystallographic twofold axis. A complete data set extending to a maximum resolution of 2.5 Å was collected at 100 K using a wavelength of 1.140 Å.

### 1. Introduction

Laccases (EC 1.10.3.2) are blue multicopper oxidases which use molecular oxygen to oxidize a great variety of phenolic compounds and aromatic amines using a radical reaction mechanism (Giardina *et al.*, 2010; Mot & Silaghi-Dumitrescu, 2012). Laccases are widely distributed in plants, insects, bacteria and especially in basidiomyceteous and ascomyceteous fungi. Their physiological roles are diverse and, in fungi, include morphogenesis, stress defence and lignin degradation.

They are useful biocatalysts for a wide range of biotechnological applications from the production of fine chemicals and pharmaceuticals to bioremediation of contaminated soil and water (Strong & Claus, 2011). They are generally monomeric glycoenzymes arranged in three  $\beta$ -barrel domains and contain two different metallic centres, which possess very distinct spectroscopic properties, in which catalysis takes place: a type 1 site (T1; paramagnetic blue copper, characterized by strong absorption at approximately 600 nm caused by a covalent copper–cysteine bond and responsible for the blue colour of these proteins), where the phenolic substrate is oxidized, and a trinuclear site, composed of one type 2 site (T2; normal copper) and one type 3 site (T3; EPR-silent antiferromagnetically coupled dinuclear coppers), which catalyzes the concomitant reduction of molecular oxygen to water using electrons received from the T1 site (see Fig. 1). All four Cu atoms are coordinated by highly conserved residues. The T1 copper ion is coordinated by two histidine N atoms and a cysteine thiolate S atom, while at the trinuclear centre the copper ions are coordinated by eight histidine residues: three for each of the T3 Cu ions and two for the T2 Cu ion.

Fungi generally express diverse isoforms of laccases encoded by complex multi-gene families (Giardina *et al.*, 2010). Among the six different laccases isolated to date from the white-rot fungus *Pleurotus ostreatus*, there are two closely related isoenzymes, POXA3a and POXA3b, that present unusual structural features since they are heterodimeric and are composed of one large subunit of 67 kDa



molecular mass and a small subunit (Palmieri *et al.*, 2003; Giardina *et al.*, 2007). The two different isoforms POXA3a and POXA3b differ by only two amino-acid substitutions in their respective small subunits. Furthermore, each small subunit is found as two different forms of molecular masses 16 and 18 kDa characterized by different degrees of glycosylation (Giardina *et al.*, 2007).

The amino-acid sequence of the large subunit is clearly homologous to other known laccase sequences and contains all of the putative copper-binding residues (Palmieri *et al.*, 2003). On the other hand, the small subunit does not show significant sequence homology to any other sequence of a protein of known function present in the databases and thus its function has still to be clarified, although a potential role of the POXA3 small subunit in the stabilization and activation of the heterodimer has been suggested (Faraco *et al.*, 2008). Recently, an additional physiological role has been hypothesized, especially during fungus fructification, in which this subunit is strongly induced while the large subunit is downregulated (Pezzella *et al.*, 2013). Some laccases endowed with a quaternary structure have also been isolated from other fungi, but most of them are homodimeric proteins. A few hetero-oligomeric laccases have been found in the fungi *Monocillium indicum* (Thakker *et al.*, 1992), *Agaricus bisporus* (Perry *et al.*, 1993) and *Armillaria mellea* (Curir *et al.*, 1997), but only limited characterization of these proteins has been reported.

In this paper, we describe the expression, purification, crystallization and preliminary crystallographic analysis of the small subunit of POXA3b (sPOXA3b) from *P. ostreatus*.

## 2. Materials and methods

### 2.1. Cloning and expression

The GenBank accession number of the sequence of the *P. ostreatus* laccase cDNA *spxoa3b* (Giardina *et al.*, 2007) reported in this paper is AM409319. *spxoa3b* cDNA was cloned into the pDEST14 recipient vector (C-terminal 6×His tag) using the Gateway cloning technology (Invitrogen). The construction was engineered in order to introduce a thrombin cleavage site between the 6×His C-terminal tag and the sequence of the protein. The forward primer was 5'-G GGG ACA AGT TTG TAC AAA AAA GCA GGC TTC GAA GGA GAT AGA ACC ATG TCA CCC TTG CAC CCA AGG CAG-3' and the reverse primer was 5'-GGG GAC CAC TTT GTA CAA GAA AGC TGG GTC TTA GTG ATG ATG ATG ATG ATG AGA ACC GCG TGG CAC TAG TGC AAA TCC GAG AGA AGC TC-3'. Expression of sPOXA3b was conducted in freshly grown *Escherichia coli* strain BL21(DE3) cells (OD 0.5–0.8) induced overnight (0.4 mM IPTG) at 290 K.

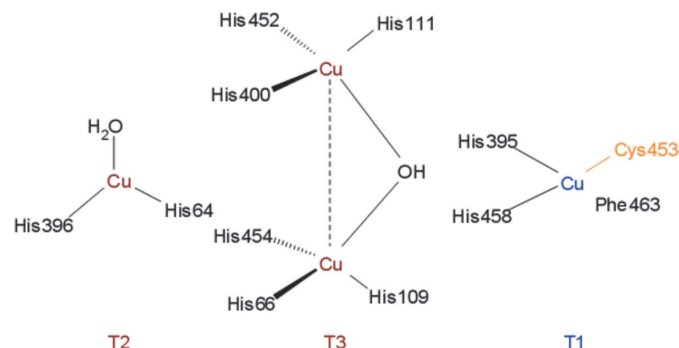


**Figure 1**  
Schematic representation of the T1, T2 and T3 copper sites of laccases.

### 2.2. Protein purification

*E. coli* cells expressing sPOXA3b were collected and pre-incubated in binding buffer (20 mM sodium phosphate, 0.5 M NaCl, 20–40 mM imidazole pH 7.4) containing lysozyme (0.3 mg ml<sup>-1</sup>) and anti-proteases (1 mM benzamidine and 1 μM leupeptin) for 4 h at 277 K. After sonication and centrifugation, the filtered supernatant was applied onto a pre-equilibrated HiTrap column (Ni-NTA). Elution was performed with a step gradient according to the manufacturer's recommendation (GE Healthcare). sPOXA3b eluted at an imidazole concentration of 300 mM. The overall yield was close to 10 mg of recombinant protein per litre. The protein was concentrated tenfold in 20 mM HEPES buffer containing 10% glycerol.

### 2.3. Crystallization

Crystallization experiments were performed using the sitting-drop vapour-diffusion method in 96-well plates (CrystalQuick, Greiner Bio-One, Germany). Drops were prepared using 1 μl protein solution mixed with 1 μl reservoir solution and were equilibrated against 100 μl precipitant solution. The protein concentration was 10.5 mg ml<sup>-1</sup> in 20 mM HEPES pH 7.0, 10% glycerol. Crystallization trials were performed using the Precipitant Synergy Primary 64 crystallization screen (Emerald BioSystems) and JBScreen Classic (Jena Bioscience, Germany) at 294 K. Hexagonal crystals were initially obtained from one condition of the Precipitant Synergy crystallization screen consisting of 20%(w/v) PEG 400, 15%(w/v) PEG 1000, 0.15 M dipotassium hydrogen phosphate/sodium dihydrogen phosphate pH 6.5. These crystals diffracted to very low resolution and all efforts to improve their quality were unsuccessful. Diffraction-quality crystals were subsequently obtained from the JBScreen Classic screen in the following range of conditions: 1.8–2.0 M sodium formate, 0.1 M Tris-HCl pH 8.5, 10–15% glycerol.

### 2.4. Data collection

A complete data set was collected on beamline ID29 at the ESRF, Grenoble from a crystal grown in 1.8 M sodium formate, 0.1 M Tris-HCl pH 8.5, 15% glycerol using a Pilatus 6M detector and a wavelength of 1.140 Å. For data collection, a crystal of the enzyme was cooled to 100 K after adding 25% glycerol as cryoprotectant to the mother-liquor solution. The data were integrated and scaled using XDS (Kabsch, 2010).

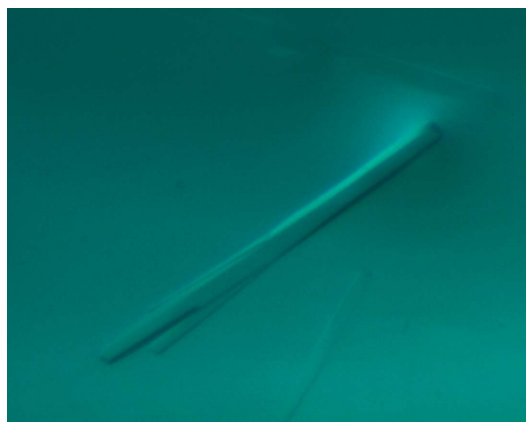


**Figure 2**  
Crystals of the small subunit of sPOXA3b grown from a solution consisting of 1.8 M sodium formate, 0.1 M Tris-HCl pH 8.5, 15% glycerol.

## 3. Results and discussion

Needle-shaped crystals of sPOXA3b from *P. ostreatus* typically grew in a few days at 294 K using the sitting-drop vapour-diffusion method to approximate dimensions of  $0.1 \times 0.1 \times 0.3$  mm (see Fig. 2). The crystals belonged to the primitive tetragonal space group  $P4_12_12$  or  $P4_32_12$ , with unit-cell parameters  $a = 126.6$ ,  $c = 53.9$  Å. Assuming the presence of two molecules of molecular mass 20.9 kDa (186 residues) in the asymmetric unit, the Matthews coefficient ( $V_M$ ) was  $2.58 \text{ \AA}^3 \text{ Da}^{-1}$ , corresponding to a solvent content of 52.4% (Matthews, 1968). The two molecules are related by a noncrystallographic twofold axis, since there are no large peaks in the native Patterson function indicative of the presence of translational pseudosymmetry, and the self-rotation function, calculated with *MOLREP* (Vagin & Teplyakov, 2010), presents a peak in the  $\kappa = 180^\circ$  section at  $\theta = 65^\circ$  and  $\varphi = 45^\circ$  with a height about 30% of that of the origin peak. Data processing gave 15 527 unique reflections, an  $R_{\text{merge}}$  of 11.5% and an overall completeness of 98.9%. Statistics of data collection

**Table 1**

Crystal parameters and data-collection statistics.

Values in parentheses are for the outermost resolution shell.

|                                          |                          |
|------------------------------------------|--------------------------|
| Beamline                                 | ID29, ESRF               |
| Wavelength (Å)                           | 1.140                    |
| Space group                              | $P4_12_12$ or $P4_32_12$ |
| Unit-cell parameters (Å)                 | $a = 126.6$ , $c = 53.9$ |
| Asymmetric unit contents                 | 2 molecules              |
| $V_M$ ( $\text{\AA}^3 \text{ Da}^{-1}$ ) | 2.58                     |
| Solvent content (%)                      | 52.4                     |
| Limiting resolution (Å)                  | 30.00–2.50 (2.65–2.50)   |
| Unique reflections                       | 15527 (2362)             |
| $R_{\text{merge}}^\dagger$ (%)           | 11.5 (61.1)              |
| $R_{\text{meas}}^\ddagger$ (%)           | 12.4 (65.8)              |
| Completeness (%)                         | 95.9 (98.9)              |
| $\langle I/\sigma(I) \rangle$            | 13.3 (2.85)              |
| Multiplicity                             | 7.3 (7.2)                |
| CC <sub>1/2</sub> (%)                    | 99.7 (90.8)              |

$\dagger R_{\text{merge}} = \sum_{hkl} \sum_i |I_i(hkl) - \langle I(hkl) \rangle| / \sum_{hkl} \sum_i I_i(hkl)$ , where  $I_i(hkl)$  is an individual intensity measurement and  $\langle I(hkl) \rangle$  is the average intensity for this reflection with summation over all data.  $\ddagger R_{\text{meas}} = \sum_{hkl} \{N(hkl)/[N(hkl) - 1]\}^{1/2} \sum_i |I_i(hkl) - \langle I(hkl) \rangle| / \sum_{hkl} \sum_i I_i(hkl)$ , where  $I_i(hkl)$  is an individual intensity measurement,  $\langle I(hkl) \rangle$  is the average intensity for this reflection with summation over all data and  $N(hkl)$  is the multiplicity.

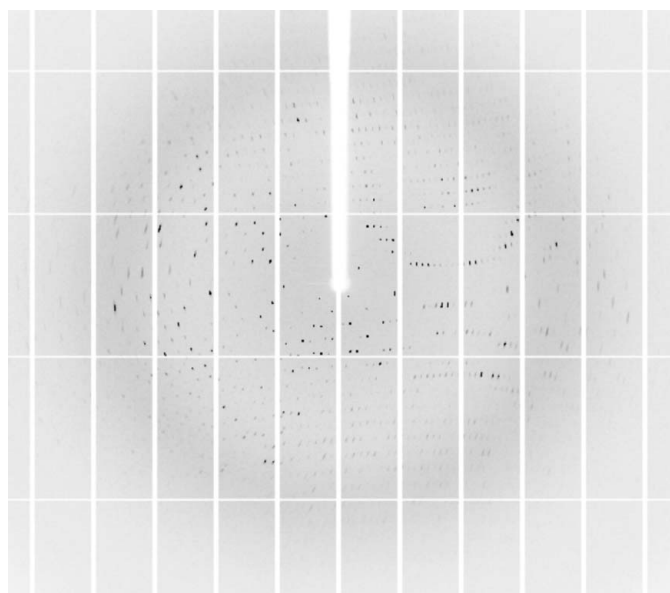


**Figure 3**  
Image showing the diffraction spots for crystals of the small subunit of POXA3b.

and processing are reported in Table 1. A diffraction image is shown in Fig. 3.

Fig. 4 reports the amino-acid sequence of sPOXA3b and the predicted secondary-structure content computed using *PSIPRED* (Jones, 1999). The sPOXA3b secondary structure is predicted to be composed of seven  $\alpha$ -helices. The sPOXA3b sequence is not closely related to any other protein of known structure. The highest similarity is to a putative enoyl-CoA hydratase/isomerase from *Acinetobacter baumannii* (PDB entry 3fdu; New York SGX Research Center for Structural Genomics, unpublished work), which shows an identity of 27.8% for 133 overlapping amino acids.

Molecular-replacement searches were performed using this 133 amino-acid fragment of the 3fdu structure and using fragments of the other two closest homologues in the Protein Data Bank, represented by PDB entries 4lq8 (Lee *et al.*, 2013) and 2hke (Byres *et al.*, 2007). The molecular-replacement trials were carried out with *MOLREP* (Vagin & Teplyakov, 2010) and *Phaser* (McCoy *et al.*, 2007), using different resolution limits and different tetragonal space groups. After unsuccessful trials using the entire protein, polyalanine models were constructed removing the amino-acid side chains. This was also not successful and did not yield better statistics than the initial searches.

Currently, attempts are being made in order to find heavy-atom derivatives and to solve the structure using their anomalous signals in a MAD or SAD experiment depending on the accessibility of the absorption-edge wavelength. Native PAGE experiments on the protein solution diluted with heavy-atom solutions as reported in

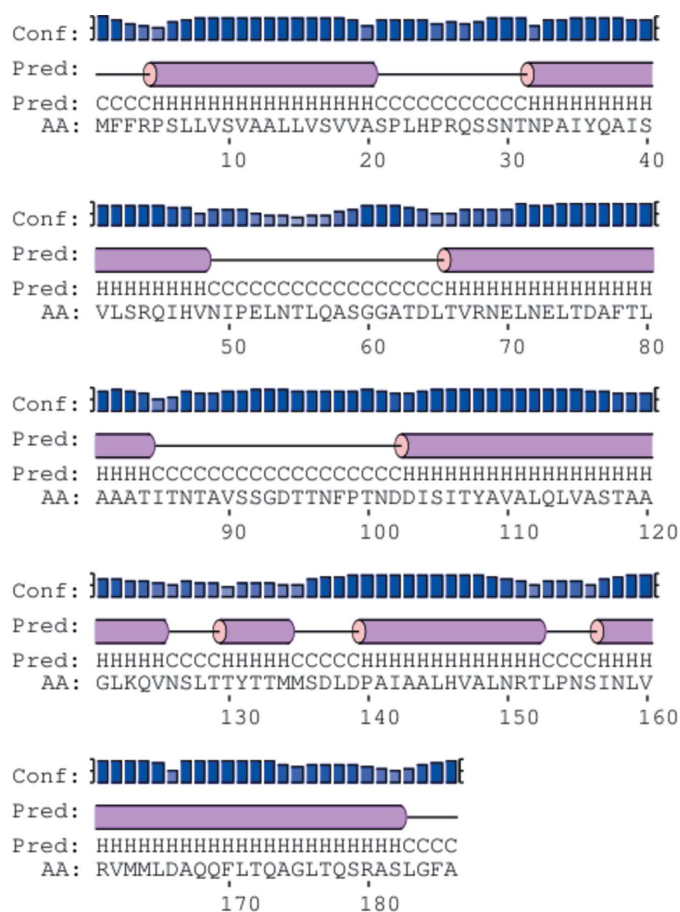


**Figure 4**  
sPOXA3b amino-acid sequence and the predicted secondary structures (C, coil; H, helix) along with the confidence of the prediction.

Boggon & Shapiro (2000) are being applied in order to pre-screen a large number of possible different compounds.

At the same time, efforts are also being made to solve the sPOXA3b structure by a method using *ab initio* prediction models as search models in molecular replacement, as implemented in the program *AMPLE* (Bibby *et al.*, 2012), which is available as part of the *CCP4* package (Winn *et al.*, 2011), as this method presents a high number of successful cases for small proteins that contain only  $\alpha$ -helices as secondary-structure elements.

The crystallographic structure of sPOXA3b, as well as that of the holoprotein, would be of invaluable importance in order to comprehend the physiological significance of the heterodimeric nature of this laccase isoform. In addition, since a stabilization role is hypothesized for this small accessory subunit, this knowledge could also provide new tools for understanding the molecular determinants that are the basis of the stability of laccases.

We acknowledge the European Synchrotron Radiation Facility for provision of synchrotron-radiation facilities and the Italian MIUR PRIN 2009 funding.

## References

- Bibby, J., Keegan, R. M., Mayans, O., Winn, M. D. & Rigden, D. J. (2012). *Acta Cryst.* **D68**, 1622–1631.
- Boggon, T. J. & Shapiro, L. (2000). *Structure*, **8**, R143–R149.
- Byres, E., Alphey, M. S., Smith, T. K. & Hunter, W. N. (2007). *J. Mol. Biol.* **371**, 540–553.
- Curir, P., Thurston, C. F., Daquila, F., Pasini, C. & Marchesini, A. (1997). *Plant Physiol. Biochem.* **35**, 147–153.
- Faraco, V., Ercole, C., Festa, G., Giardina, P., Piscitelli, A. & Sannia, G. (2008). *Appl. Microbiol. Biotechnol.* **77**, 1329–1335.
- Giardina, P., Autore, F., Faraco, V., Festa, G., Palmieri, G., Piscitelli, A. & Sannia, G. (2007). *Appl. Microbiol. Biotechnol.* **75**, 1293–1300.
- Giardina, P., Faraco, V., Pezzella, C., Piscitelli, A., Vanhulle, S. & Sannia, G. (2010). *Cell. Mol. Life Sci.* **67**, 369–385.
- Jones, D. T. (1999). *J. Mol. Biol.* **292**, 195–202.
- Kabsch, W. (2010). *Acta Cryst.* **D66**, 125–132.
- Lee, J. H., Vonnrhein, C., Bricogne, G. & Izard, T. (2013). *Protein Sci.* **22**, 1425–1431.
- Matthews, B. W. (1968). *J. Mol. Biol.* **33**, 491–497.
- McCoy, A. J., Grosse-Kunstleve, R. W., Adams, P. D., Winn, M. D., Storoni, L. C. & Read, R. J. (2007). *J. Appl. Cryst.* **40**, 658–674.
- Mot, A. C. & Silaghi-Dumitrescu, R. (2012). *Biochemistry (Mosc.)*, **77**, 1395–1407.
- Palmieri, G., Cennamo, G., Faraco, V., Amoresano, A., Sannia, G. & Giardina, P. (2003). *Enzyme Microb. Technol.* **33**, 220–230.
- Perry, C. R., Matcham, S. E., Wood, D. A. & Thurston, C. F. (1993). *J. Gen. Microbiol.* **139**, 171–178.
- Pezzella, C., Lettera, V., Piscitelli, A., Giardina, P. & Sannia, G. (2013). *Appl. Microbiol. Biotechnol.* **97**, 705–717.
- Strong, P. J. & Claus, H. (2011). *Crit. Rev. Environ. Sci. Technol.* **41**, 373–434.
- Thakker, G. D., Evans, C. S. & Rao, K. K. (1992). *Appl. Microbiol. Biotechnol.* **37**, 321–323.
- Vagin, A. & Teplyakov, A. (2010). *Acta Cryst.* **D66**, 22–25.
- Winn, M. D. *et al.* (2011). *Acta Cryst.* **D67**, 235–242.